Numerical Solutions of the Percus–Yevick Equation for the Lennard-Jones (6–12) and Hard-Sphere Potentials

Frederic Mandel, Richard J. Bearman, and Mirion Y. Bearman

Articles you may be interested in

Numerical Solutions of the Percus—Yevick Equation for the Hard-Sphere Potential
The Journal of Chemical Physics **42**, 2408 (1965); 10.1063/1.1696308

Equation of State for Hard Spheres
The Journal of Chemical Physics **39**, 474 (1963); 10.1063/1.1734272

Direct correlation function: Hard sphere fluid
The Journal of Chemical Physics **63**, 601 (1975); 10.1063/1.431378

Analytic Solution of the Percus-Yevick Equation
Journal of Mathematical Physics **5**, 643 (1964); 10.1063/1.1704158

Radial Distribution Functions and the Equation of State of Fluids Composed of Molecules Interacting According to the Lennard-Jones Potential
The Journal of Chemical Physics **20**, 929 (1952); 10.1063/1.1700653

Percus-Yevick Equation Applied to a Lennard-Jones Fluid
The Journal of Chemical Physics **48**, 50 (1968); 10.1063/1.1667953

Numerical Solutions of the Percus–Yevick Equation for the Lennard-Jones (6–12) and Hard-Sphere Potentials

FREDERIC MANDEL

Department of Chemistry, University of Kansas, Lawrence, Kansas 66044

AND

RICHARD J. BEARMAN, AND MIRION Y. BEARMAN

Department of Chemistry, University of Kansas, Lawrence, Kansas 66044 and Department of Physical and Inorganic Chemistry,
University of New England, Armidale, NSW 2351, Australia

(Received 18 September 1969)

Numerical solutions of the Percus–Yevick equation for the Lennard-Jones (6–12) potential are presented largely for high densities and the liquid region in a form particularly useful to workers who have access only to small computers which cannot be used for solving the PY equation. The solutions, given in a form suitable for calculating either the radial distribution functions or direct correlation functions, are deposited with the National Auxiliary Publications Service (Document No. NAPS-00720). A table of densities and temperatures at which the PY solutions are available is given. Energies and pressures, including the compressibility pressure for temperatures below the critical, are also tabulated and comparisons are made with molecular dynamics results. Solutions for the hard-sphere potential are also presented completing the tables of Throop and Bearman [J. Chem. Phys. **43**, 2408 (1965)] for large intermolecular separations.

I. INTRODUCTION

At the moment, perturbation theories such as the Barker–Henderson theory[1] appear to be the most successful theories for understanding the thermodynamic properties of dense fluids and liquids. Thus far, however, they have not yielded correlation functions, which are of interest both in their own right[2] and in the calculation of transport properties,[3] besides providing alternative routes to the thermodynamic properties.[4]

A. Percus–Yevick Lennard-Jones (6–12) Correlation Functions

Correlation functions are conveniently calculated from integral equations, and of these, the Percus–Yevick equation[5,6] has proved to be one of the best. Although the results of a considerable number of calculations have been published[5,6,7] the correlation functions themselves have not been extensively tabulated for the Lennard-Jones potential at high densities, especially in the liquid region. Furthermore, the available tables mainly provide radial distribution functions, which cannot be converted accurately to the shorter-

ranged direct correlation functions in the most interesting region of small intermolecular separations.

We have tried to remedy these deficiencies of the literature by depositing an extensive tabulation of the function $h(r)$ (defined in Sec. II) with the National Auxiliary Publications Service.[8] The densities and temperatures for which h is available are listed. Especially noteworthy is the rather large selection of points in the liquid region. The function h, which is the direct solution of the PY integral equation, can be converted readily and rapidly, even on small computers, to either the radial distribution function or the direct correlation function. For convenience, we also tabulate virial pressures, compressibilities and compressibility pressures, and energies calculated from the correlation functions.

In Sec. III, we compare some of our results with molecular dynamics data obtained by Verlet.[9] We see that even in the liquid region the PY distribution function and energy provide fairly good approximations to the correct values. As several authors have indicated,[10] the Percus–Yevick equation does not predict pressures with accuracy in the liquid region, but poor as they are, the compressibility and virial pressures still bracket the true pressure.[5] It is our opinion, therefore, that it is

3315

something of an overstatement to assert that the Per-cus–Yevick theory is unsatisfactory in the liquid state[11]; its degree of adequacy depends upon the use to which it is put.

B. Percus–Yevick Hard-Sphere Distribution Functions

In an earlier paper, Throop and Bearman[12] tabulated hard-sphere Percus–Yevick radial distribution functions for intermolecular separations up to 3.95. The usefulness of these distribution functions[1] has made desirable an extension of the tables to larger distances. In order to complete the tables, we list in Sec. IV the hard-sphere distribution functions from 4.00–6.00.

II. SOLUTIONS OF THE PERCUS–YEVICK EQUATION FOR THE LENNARD-JONES 6–12 POTENTIAL

A. Radial Distribution Functions

If the Percus–Yevick approximation

$$c(r) = g(r)\{1 - \exp[\beta u(r)]\} \quad (II.1)$$

is combined with the Ornstein–Zernike definition of the direct correlation function $c(r)$,

$$G(r) \equiv g(r) - 1 = c(r) + \rho \int c(r')G(|r-r'|)dr', \quad (II.2)$$

where $\beta = 1/kT$, ρ is the number density, and $u(r)$ the intermolecular potential, then one obtains an integral equation for the radial distribution function $g(r)$. It is expedient to solve this equation by a method due to Broyles.[13] Defining

$$h(r) \equiv rg(r) \exp[\beta u(r)] \quad (II.3)$$

enables Eqs. (II.1) and (II.2) to be written in the following form:

$$h' = 1 - 2\pi\rho \int_0^\infty \{1 - \exp[-\beta u(s)]\}h(s)$$

$$\times \{h(s+r) \exp[-\beta u(s+r)]$$

$$+ h(|s-r|) \exp[-\beta u(|s-r|)]$$

$$\times [(s-r)/|s-r|] - 2s\}ds, \quad (II.4)$$

$$h(r) = \int_0^r h'(t)dt. \quad (II.5)$$

In the detailed solutions, it is convenient to introduce the following dimensionless quantities:

$$r^* = r/\sigma, \qquad T^* = kT/\epsilon, \qquad \rho^* = \rho\sigma^3. \quad (II.6)$$

Starting with a trial h, we iterate until a self-consistent h is obtained. If we call a first input value of h, "h_{in}(old)" and call the resultant output value, "h_{out}," then the new input, "h_{in}(new)," is given by

$$h_{in}(new) = \alpha h_{in}(old) + (1-\alpha)h_{out}, \quad (II.7)$$

with $0 < \alpha < 1$. In their paper[5a] Throop and Bearman

used the following convergence criterion,

$$\epsilon \equiv |h_{in}(new) - h_{in}(old)| = (1-\alpha)\epsilon' \lesssim 10^{-5}, \quad (II.8)$$

with

$$\epsilon' \equiv |h_{in}(old) - h_{out}|. \quad (II.9)$$

Since we have an exact solution when $\epsilon' = 0$, regardless of α, it is better to state the convergence criterion in terms of ϵ' when α is near unity. This is the case at high densities where values of α as high as 0.95 have to be used even if the initial trial h is for a system very close in density (e.g., $\Delta\rho^* = 0.01$) to the system for which h is desired. We have used a convergence criterion, $\epsilon' < 10^{-4}$ in this paper. Otherwise, the technique of Throop and Bearman was not altered.

The calculations in this section were carried out with the Lennard-Jones 6–12 potential,

$$u(r) = 4\epsilon[(\sigma/r)^{12} - (\sigma/r)^6]. \quad (II.10)$$

B. Thermodynamic Functions

The thermodynamic functions can be expressed in terms of the radial distribution functions with the following equations[4,14]:

$$\frac{\beta E}{N} = \frac{3}{2} + 2\pi\rho \int_0^\infty r^2 \beta u(r)g(r)dr, \quad (II.11)$$

$$\frac{\beta P}{\rho} = 1 - \frac{2\pi\rho}{3} \int_0^\infty r^3 \beta \frac{du(r)}{dr} g(r)dr, \quad (II.12)$$

$$\beta\left(\frac{\partial P}{\partial \rho}\right)_T = 1 - 4\pi\rho \int_0^\infty c(r)r^2 dr. \quad (II.13)$$

When integrated from zero density to the density of interest, Eq. (II.13) yields the compressibility pressure (P^c) which may then be compared with the virial pressure (P^v) obtained from (II.12). When the two phase region intervenes, direct integration is not practicable. Hence, below the critical point it is necessary to use the following formulation recently proposed by Baxter in the Percus–Yevick approximation[15]:

$$\frac{\beta P^c}{\rho} = 1 + 2\pi\rho \int_0^\infty r^2 c(r) \left\{\frac{c(r)}{1 - \exp[u(r)/kT]} - 2\right\} dr$$

$$+ (2\pi^2\rho)^{-1} \int_0^\infty k^2 \{\log[1 - \rho\hat{c}(k)] + \rho\hat{c}(k)\}dk, \quad (II.14)$$

where

$$\hat{c}(k) = \frac{4\pi}{k} \int_0^\infty rc(r) \sin(kr)dr. \quad (II.15)$$

The first integral in Eq. (II.14) may be rewritten as

$$I_1 = 2\pi\rho \int_0^\infty r^2 c(r)[g(r) - 2]dr \quad (II.16)$$

in the Percus–Yevick approximation.

Using Simpson's rule, we have evaluated the integrals

in Eqs. (II.11)–(II.13) and (II.16) for the same range as used to calculate $h(r)$. The asymptotic part of the integral was evaluated analytically after setting $g(r)=1$ and $c(r)=-\beta u(r)$. In the integration, we have found it efficacious to use a grid spacing half that used to obtain $h(r)$. By interpolating $h(r)$ [and consequently $g(r)$ and $c(r)$] at the halfway points and using these points to calculate the thermodynamic functions, we get results close to those obtained by using the finer grid spacing in the Percus–Yevick equation.

The error[5b] associated with Eqs. (II.11)–(II.13) is estimated to be ±0.0004 at temperatures near the critical temperature. Eq. (II.14) was evaluated using Simpson's rule. Because the two integrals in Eq. (II.14) are almost equal in magnitude but of opposite sign, they must both be evaluated very accurately. We found that the largest source of error lies in the numerical evaluation of the second integral in Eq. (II.14). In Table I we have tabulated the value of that integral as a function of the grid spacing, while in Table II the

TABLE I. The second compressibility integral vs grid spacing.

Grid spacing	Value of the integral[a]
0.20	160.490
0.18	160.488
0.15	160.487
0.09	160.486
0.05	160.486

[a] The upper limit of integration was 200. The reduced density $\rho^*=0.75$ and the reduced temperature $T^*=1.062$.

effect of truncating the integral at different points is listed. On the basis of these calculations, a grid spacing of 0.09 and an upper limit of $k=180$ were used to evaluate the integral. Equation (II.15) was evaluated at the same points using Filon's Method.[16] Some compressibility pressures calculated by using Eq. (II.14) above the critical temperature are compared in Table III with those obtained by integrating Eq. (II.13) with respect to the density. We estimate the error in the former to be ±0.001 and ±0.0002 in the latter.

At liquid argon temperatures, the error in the thermodynamics properties is generally greater for two reasons. First, larger convergence criteria are used at the low temperatures (cf. Table IVl).[16] Second, the correlation functions are longer ranged and oscillate more rapidly at low temperatures so that integration errors are larger for a fixed grid spacing. Although we have not carried out as systematic an error analysis at liquid argon temperatures as we have carried out at temperatures near the critical point, on the basis of our experience with the PY equation, we estimate the error in the pressures and the inverse compressibility to be ±0.005 and the error in the energy to be ±0.002.

TABLE II. The value of the second integral as a function of the upper limit of integration.

Upper limit	Value of the integral
180	160.486
135	160.486
90	160.485
67.5	160.484
45	160.470
22.5	159.115

C. Scope of the Calculations

As mentioned in the Introduction, we have tabulated $h(r)\equiv rg(r)\exp[\beta u(r)]$ rather than $g(r)$ itself. These tabulations are given in Tables IVa–IVk deposited with NAPS.[8] The densities and temperatures at which $h(r)$ has been calculated are presented in Table IVl and are graphically depicted in Fig. 1. Table IVl also contains the grid spacings, ranges and the convergence criteria used in the calculation. In Table IVm we have listed $h(r)$ for $\rho^*=0.85$ and $T^*=0.88$. These may be compared with the molecular dynamics calculation of Verlet.[9b] The reader may note that $h(r)$ is a far smoother function than $g(r)$ and therefore is more amenable to interpolation. The radial distribution function $g(r)$ may be obtained from the definition of $h(r)$. The direct correlation function is given by Eq. (II.1) and can be written as:

$$c(r)=r^{-1}\{\exp[-\beta u(r)]-1\}h(r). \quad (II.17)$$

in Tables V.A and V.B we give the values of P^v and P^c as calculated from Eqs. (II.12) and (II.14), respectively.

We have listed the internal energy in Table V.C and the inverse compressibility in Table V.D.

D. Comparison with the Results of Throop and Bearman

Tables V.A–V.C of this paper overlap at some points with Tables IIb, 2c, and IIIa of the paper by Throop and Bearman. The virial pressures and the inverse compressibilities agree at all points to within ±0.0002. The residual discrepancy is probably due to the slightly better convergence criteria used in this paper and to

TABLE III. Comparison of the pressures obtained by integrating $\beta dP/d\rho$ and by using Baxter's equation.

T^*	ρ^*	$\beta P^c/\rho^*$ [a]	$\beta P^c/\rho^*$ [b]
1.35	0.10	0.7182	0.7180
1.35	0.15	0.6006	0.6000
1.35	0.45	0.3086	0.3077
1.40	0.45	0.3796	0.3790
1.40	0.55	0.5064	0.5067
1.40	0.60	0.6374	0.6379

[a] Compressibility pressure obtained by integrating $\beta dP/d\rho$ with respect to the density.
[b] Pressure obtained from Eq. (II.14).

TABLE IV. Correlation functions.

IVL. Values of $\epsilon' \times 10^5$ used in Tables IVa–IVk[a,b]

$\rho^* \backslash T^*$	2.63	2.21	1.78	1.5	1.4	1.35	1.20	1.0718	1.062	0.9182	0.75126
0.20	0.7	0.6	0.6	0.6	8.5						
0.30	0.9	0.6	0.9		8.2						
0.40	0.8	0.2	0.2	7.3	6.7						
0.45				1.6	0.8	6.2					
0.50	5.3	0.8	0.8		8.5						
0.60					0.7	9.3	9.6[d]	9.4[d]	1.1[e]	9.6[e]	
0.65	8.8[e]	9.0[e]	6.1[e]		8.5		19.6[d]		1.1[e]	9.9[e]	
0.70									1.2[e]	9.9[e]	9.1[d]
0.75	9.5[e]	7.7[e]	7.3[e]		1.6[e]				1.9[e]	9.9[e]	9.4[d]
0.80							9.8[e]		2.8[e]	8.4[e]	
0.8152	3.9[e]	5.1[e]	9.5[e]		3.5[e]		3.3[e]		9.4[e]		5.6[e], 9.6[d]
0.85	4.5[e]	9.4[e]	9.4[e]		9.4[e]		9.7[e]		4.0[e]	12.8[e]	
0.90									5.4[e]		
0.925											9.6[e]

IV.M. Tabulation of $h(r) = rg(r) \exp[\beta u(r)]$

Reduced temperature = 0.88   Reduced density = 0.85

r^*	$h(r^*)$	r^*	$h(r^*)$	r^*	$h(r^*)$
0.05	1.28331	2.05	2.48695	4.05	4.06141
0.10	2.42047	2.10	2.50338	4.10	4.07562
0.15	3.31107	2.15	2.40895	4.15	4.09439
0.20	3.97787	2.20	2.24838	4.20	4.12019
0.25	4.47057	2.25	2.10203	4.25	4.15687
0.30	4.81368	2.30	1.99624	4.30	4.20512
0.35	5.04182	2.35	1.95554	4.35	4.26464
0.40	5.16306	2.40	1.97521	4.40	4.33387
0.45	5.19413	2.45	2.04173	4.45	4.40877
0.50	5.13853	2.50	2.14551	4.50	4.48683
0.55	5.00802	2.55	2.26967	4.55	4.56319
0.60	4.80557	2.60	2.40736	4.60	4.63589
0.65	4.54280	2.65	2.54701	4.65	4.70188
0.70	4.22342	2.70	2.68437	4.70	4.76052
0.75	3.86052	2.75	2.81226	4.75	4.81138
0.80	3.45933	2.80	2.92794	4.80	4.85502
0.85	3.03594	2.85	3.02658	4.85	4.89311
0.90	2.59856	2.90	3.10610	4.90	4.92690
0.95	2.16883	2.95	3.16274	4.95	4.95907
1.00	1.75933	3.00	3.19501	5.00	4.99102
1.05	1.39304	3.05	3.20185	5.05	5.02534
1.10	1.08132	3.10	3.18586	5.10	5.06304
1.15	0.83503	3.15	3.15763	5.15	5.10573
1.20	0.65678	3.20	3.12624	5.20	5.15370
1.25	0.54066	3.25	3.10960	5.25	5.20698
1.30	0.48302	3.30	3.11409	5.30	5.26500
1.35	0.47087	3.35	3.14689	5.35	5.32625
1.40	0.50064	3.40	3.20667	5.40	5.38963
1.45	0.56081	3.45	3.28750	5.45	5.45289
1.50	0.64951	3.50	3.38429	5.50	5.51498
1.55	0.75858	3.55	3.48696	5.55	5.57409
1.60	0.88751	3.60	3.59092	5.60	5.62973
1.65	1.03101	3.65	3.68843	5.65	5.68133
1.70	1.18940	3.70	3.77695	5.70	5.72907
1.75	1.35958	3.75	3.85278	5.75	5.77366
1.80	1.54232	3.80	3.91533	5.80	5.81576
1.85	1.73620	3.85	3.96449	5.85	5.85679
1.90	1.94187	3.90	4.00111	5.90	5.89752
1.95	2.15383	3.95	4.02775	5.95	5.93935
2.00	2.35743	4.00	4.04635	6.00	5.98282

[a] Lack of a superscript indicates that a grid spacing of 0.05σ and an integral cutoff of 6.0σ was used.

[b] The $h(r)$'s for several isolated points are given in Tables IVa–IVk but are not listed above. These points are: $\rho^* = 0.8158$, $T^* = 0.7513$[d]; $\rho^* = 0.85$, $T^* = 0.88$[e]; $\rho^* = 0.8887$, $T^* = 0.7646$[e]; $\rho^* = 0.8886$, $T^* = 0.7513$[e]; $\rho^* = 0.8750$, $T^* = 0.6928$[e]; $\rho^* = 0.25$, $T^* = 1.5$; $\rho^* = 0.55$, $T^* = 1.4$; $\rho^* = 0.10$, $T^* = 1.35$; $\rho^* = 0.15$, $T^* = 1.35$. The first five points were calculated with $\epsilon' \simeq 10^{-4}$, while for the last four points $\epsilon' \simeq 10^{-5}$.

[c] A grid spacing of 0.05σ and an integral cutoff of 7.5σ was used.

[d] A grid spacing of 0.02σ and an integral cutoff of 8.0σ was used in the PY equation, but the results are tabulated at a grid spacing of 0.04σ.

[e] A grid spacing of 0.04σ and an integral cutoff of 8.0σ was used.
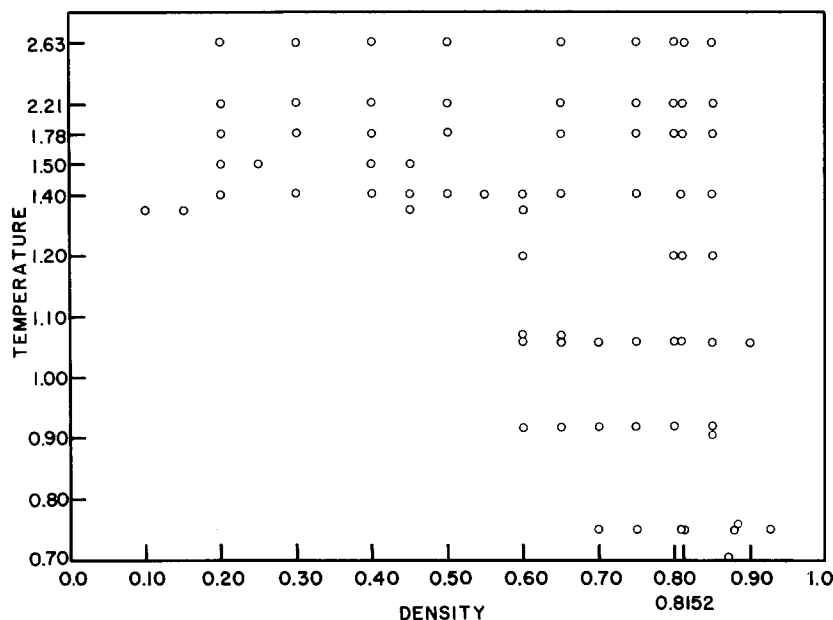
FIG. 1. Densities and temperatures at which the Percus–Yevick equation was evaluated.

the correction of two slight errors in the program used to calculate the thermodynamic properties. The errors were generally found to contribute only in the fifth or sixth decimal place but could conceivably cause an error of one in the fourth decimal place. The agreement in the energy is also within ±0.0002 except at $\rho^*=0.20$ and $\rho^*=0.30$ at $T^*=1.4$ where the errors are unaccountably larger.

As we have mentioned in Sec. II.B, Throop and Bearman interpolated $g(r)$ before calculating the virial pressure, energy, and inverse compressibility. In a sample calculation made in the course of preparation of another paper,[5b] we found for a Lennard-Jones potential truncated past 6σ: Integration without interpolation yields a value of 0.3925 for the inverse compressibility at $T^*=1.40$ and $\rho^*=0.40$, while with interpolation a value of 0.3897 is obtained. Both these values are for a grid spacing of 0.05σ. When the Percus–Yevick equation is solved with a grid spacing of 0.025σ and the resulting direct correlation function is integrated without interpolation we obtain a value of 0.3896 for the inverse compressibility. It follows that interpolation is very desirable in these cases, and we have continued the practice.

A separate program was used by Throop and Bearman to calculate the compressibility pressures and in this program interpolation was not used. To gauge the error, we note that at $T^*=1.40$ and $\rho^*=0.60$, the compressibility pressure has a value of 0.6442 without interpolation and a value of 0.6374 with interpolation. Therefore the compressibility pressures and presumably the corresponding entropies given in the paper by Throop and Bearman should be used with care. If more accurate results are needed the inverse compressibilities should be integrated using interpolation at halfway

points. Interpolation was used in the preparation of Table VB of this paper.

III. COMPARISON WITH MOLECULAR DYNAMICS

Although the Percus–Yevick equation may be considered an adequate approximate theory of simple fluids for densities up to $1\frac{1}{2}$ times the critical density,[5a,6] a systematic study of the Percus–Yevick equation has not been previously made for temperatures and densities in the liquid region. Nevertheless, the consensus[10,11] of opinion has been that the PY equation is inadequate in the liquid region. The main basis for that opinion is the poor agreement of the virial pressure (P^v) with experimental results. However, for several reasons, this should not be used as the sole criterion for judging the PY equation: First, from comparisons above the critical temperature,[5a] it is known that the compressibility pressure (P^c) is superior to the virial pressure (P^v). Thus, the compressibility pressure also ought to be compared with experiment below the critical point. In the past no such comparisons were made because no method was known for calculating P^c below the critical temperature. However, Baxter[15] has recently demonstrated how to make the calculation, so that ignorance is no longer a valid excuse. Second, the pressure is not the only property of interest. Comparisons with other properties, such as the energy and correlation functions, should also be given strong consideration in any assessment of the value of the PY equation. Third, comparisons with data on real substances are of doubtful value because real fluids do not obey the Lennard-Jones potential with exactitude.[6] Hence, one should compare Percus–Yevick results with molecular dynamics[9] calculations.

TABLE V. Thermodynamic properties for the Percus-Yevick approximation.

ρ^* \ T^*	2.63	2.21	1.78	1.40	1.20	1.071	1.062	0.9182	0.75126
A. Values of $P^v/\rho kT$									
0.20	0.9746	0.887	0.7532	0.5488					
0.30	1.045	0.919	0.7276	0.4462					
0.40	1.203	1.044	0.8006	0.4476					
0.50	1.486	1.303	1.020	0.6052					
0.55				0.7702					
0.60				1.009	0.660	0.370	0.346	−0.06	
0.65	2.248	2.068	1.779	1.337		0.680	0.671	0.252	
0.70							1.126	0.717	0.097
0.75	3.068	2.932	2.696	2.318			1.732	1.36	0.782
0.80					2.75		2.51	2.19	
0.8152	3.776	3.694	3.529	3.243	3.00		2.78		2.04
0.85	4.219	4.176	4.063	3.845	3.65		3.48	3.24	
0.90							4.67		
B. Values of $P^c/\rho kT$									
0.20	0.9732	0.8837	0.7472	0.5389					
0.30	1.033	0.9027	0.7051	0.4118					
0.40	1.164	0.9963	0.7391	0.3663					
0.50	1.404	1.196	0.8800	0.4238					
0.55				0.5064					
0.60				0.6374	0.229	−0.1	−0.15	−0.6	
0.65	2.06	1.810	1.413	0.828		0.01	−0.02	−0.5	
0.70				1.09			0.18	−0.4	−1.2
0.75	2.81	2.547	2.113	1.45			0.48	−0.1	−1.0
0.80					1.38		0.89	0.23	
0.8152	3.49	3.23	2.79	2.10	1.55		1.04		−0.63
0.85	3.93	3.69	3.25	2.55	1.97		1.45	0.75	
0.90							2.19		
C. Values of $\beta E_i/N$									
0.20	−0.4625	−0.5767	−0.7582	−1.0663					
0.30	−0.6867	−0.8527	−1.1107	−1.5293					
0.40	−0.9077	−1.1253	−1.4565	−1.9600					
0.50	−1.1236	−1.3945	−1.8016	−2.3995					
0.55				−2.6235					
0.60				−2.8476	−3.403	−3.878	−3.918	−4.645	
0.65	−1.4231	−1.7770	−2.3054	−3.0689		−4.180	−4.216	−4.975	
0.70							−4.514	−5.320	−6.66
0.75	−1.5904	−1.9992	−2.6093	−3.4892			−4.803	−5.662	−7.08
0.80					−4.411		−5.078	−5.990	
0.8152	−1.6772	−2.1200	−2.7815	−3.7354	−4.479		−5.158		−7.61
0.85	−1.7143	−2.1743	−2.8619	−3.854	−4.627		−5.333	−6.298	
0.90							−5.561		
D. Values of $[kT(\partial\rho/\partial P)_T]^{-1}$									
0.20	1.030	0.8586	0.5985	0.2100					
0.30	1.303	1.053	0.6791	0.1487					
0.40	1.871	1.546	1.056	0.3675					
0.50	2.902	2.515	1.913	1.047					
0.55				1.662					
0.60				2.538	1.743	1.092	1.036	0.1475	
0.65	5.925	5.526	4.837	3.751		2.159	2.108	1.084	
0.70							3.633	2.499	7.50
0.75	9.58	9.30	8.69	7.59			5.74	4.51	2.55
0.80					9.53		8.60	7.29	
0.8152	13.1	12.9	12.5	11.5	10.6		9.65		6.12
0.85	15.4	15.4	15.2	14.3	13.4		12.4	11.1	
0.90							17.5		

As a test of the PY equation, we have tabulated the PY virial and compressibility pressures and the molecular dynamics pressure. We also compare the PY and molecular dynamics internal energies (E_i) and radial distribution functions $g(r)$. The thermodynamic properties are given in Table VI while the distribution functions are shown in Fig. 2.

It is evident from Table VI that the PY equation is incapable of yielding quantitative virial and compressibility pressures in the liquid region. The large

TABLE VI. Comparison of the Percus-Yevick and molecular dynamics thermodynamic properties.

T^*	ρ^*	Pressure ($\beta P/\rho$)			Energy ($\beta E_i/N$)	
		Percus-Yevick P^c	Molecular dynamics	Percus-Yevick P^v	Molecular dynamics	Percus-Yevick
0.880	0.85	0.54	1.64	3.17	−6.75	−6.61
0.786	0.85	(−0.10)	0.99	2.97	−7.70	−7.51
0.719	0.85	(−0.60)	0.36	2.82	−8.51	−8.28
1.128	0.85	1.71	2.78	3.57	−5.05	−4.98

discrepancy between the virial and compressibility equations of state is in itself a measure of the error involved. Both PY equations of state differ from the molecular dynamics pressures by more than 100%. The two results do bracket the molecular dynamics results, however, and it is interesting to note that in the two cases where P^c is not negative the simple arithmetic mean is only off by about 10%.

The pressure is extremely sensitive to small errors in the correlation functions, and one might expect the PY energy to be better. Such is the case, for the error in the energy is approximately 2.5% at the lowest temperature and tends to decrease for higher temperatures.

From Fig. 2, we see that the form of the PY and molecular dynamics radial distribution functions are quite similar. The first peak of the Percus-Yevick $g(r)$ is slightly broader and higher than the molecular dynamics peak and the PY first maximum and minimum occur at smaller values of r^*, but on the whole the agreement between the two is quite good.

We conclude that the PY equation should be used only with great caution to estimate pressures below the critical point, but it does represent fairly well the distribution functions and energies.
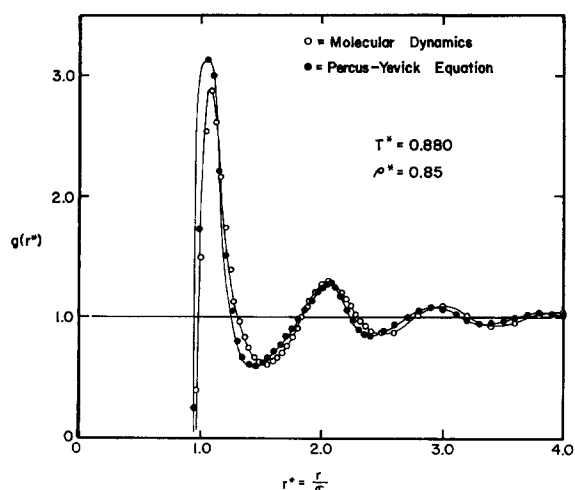

FIG. 2. The pair distribution function $g(r)$ as a function of r^* for $T^*=0.88$ and $\rho^*=0.85$. The solid circles are results obtained from the PY equation. The open circles are molecular dynamics results.

IV. HARD-SPHERE DISTRIBUTION FUNCTIONS

Using the method suggested by Wertheim,[17] which involves the use of Laplace transforms, Throop and Bearman have evaluated the PY radial distribution function $g(r)$ for $\sigma \leq r < 4\sigma$, where σ is the hard-sphere diameter.[12] While exact, this method becomes increasingly unwieldy as r increases. Hence, we have used a different approach.

The direct correlation function for hard-spheres may be written

$$c(r^*) = -\lambda_1 - 6\eta\lambda_2 r^* - 1/2\eta\lambda_1 r^{*3} \quad \text{for} \quad r^* \equiv r/\sigma \leq 1,$$
(IV.1)

where,

$$\lambda_1 = (1+2\eta)^2/(1-\eta)^4,$$
(IV.2)

$$\lambda_2 = -\frac{(1-\frac{1}{2}\eta)^2}{(1-\eta)^4},$$
(IV.3)

and

$$\eta = \pi\rho\sigma^3/6.$$
(IV.4)

For $r^* > 1$,

$$c(r^*) = 0.$$
(IV.5)

Taking the three-dimensional Fourier transform of Eq. (II.2) and utilizing the convolution theorem we find

$$\widehat{G}(k) = \hat{c}(k) + \rho\hat{c}(k)\widehat{G}(k),$$
(IV.6)

where $\widehat{G}(k)$ and $\hat{c}(k)$ are the Fourier transforms of $G(r)$ and $c(r)$ respectively. Then

$$\widehat{G}(k) = \hat{c}(k)/[1-\rho\hat{c}(k)].$$
(IV.7)

The right-hand side of Eq. (IV.7) is obtained analytically, and then the transform $\widehat{G}(k)$ is numerically inverted to give $G(r)$.

Writing

$$\hat{c}(k) = \hat{c}_1(k) + \hat{c}_2(k) + \hat{c}_3(k),$$

where $\hat{c}_1$, $\hat{c}_2$, $\hat{c}_3$ are, respectively, the three-dimensional Fourier transforms of the three terms in Eq. (IV.1), and using the relation

$$\hat{c}(k) = 4\pi \int_0^1 \frac{\sin kr^*}{kr^*} r^{*2} c(r^*) dr^*,$$
(IV.8)

TABLE VII. Hard-sphere radial distribution functions.

Density	0.5000	0.6000	0.7000	0.8000	0.9000	1.0000	1.1000
R^*				$g(r^*)$			
4.000	0.99899	0.99963	1.00577	1.01920	1.02503	0.98709	0.89583
4.050	0.99932	1.00064	1.00702	1.01720	1.01315	0.96481	0.88457
4.100	0.99964	1.00145	1.00742	1.01357	1.00062	0.94764	0.88749
4.150	0.99994	1.00200	1.00703	1.00884	0.98891	0.93761	0.90492
4.200	1.00019	1.00228	1.00599	1.00364	0.97937	0.93582	0.93502
4.250	1.00038	1.00231	1.00449	0.99858	0.97298	0.94222	0.97356
4.300	1.00051	1.00212	1.00273	0.99421	0.97024	0.95556	1.01469
4.350	1.00056	1.00176	1.00093	0.99091	0.97117	0.97366	1.05210
4.400	1.00056	1.00130	0.99926	0.98893	0.97534	0.99383	1.08033
4.450	1.00052	1.00079	0.99788	0.98833	0.98195	1.01331	1.09573
4.500	1.00043	1.00028	0.99688	0.98901	0.99001	1.02967	1.09697
4.550	1.00032	0.99982	0.99631	0.99077	0.99847	1.04111	1.08493
4.600	1.00021	0.99944	0.99617	0.99330	1.00634	1.04666	1.06239
4.650	1.00009	0.99917	0.99642	0.99626	1.01279	1.04614	1.03327
4.700	0.99999	0.99902	0.99698	0.99930	1.01726	1.04014	1.00200
4.750	0.99991	0.99897	0.99776	1.00209	1.01942	1.02984	0.97277
4.800	0.99984	0.99903	0.99867	1.00439	1.01926	1.01679	0.94906
4.850	0.99981	0.99917	0.99960	1.00600	1.01699	1.00272	0.93333
4.900	0.99979	0.99936	1.00045	1.00684	1.01304	0.98932	0.92682
4.950	0.99980	0.99958	1.00116	1.00688	1.00797	0.97806	0.92964
5.000	0.99982	0.99981	1.00167	1.00620	1.00242	0.97008	0.94089
5.050	0.99985	1.00003	1.00196	1.00494	0.99704	0.96611	0.95880
5.100	0.99989	1.00021	1.00202	1.00329	0.99240	0.96637	0.98103
5.150	0.99994	1.00034	1.00188	1.00146	0.98896	0.97062	1.00478
5.200	0.99998	1.00043	1.00156	0.99965	0.98704	0.97815	1.02709
5.250	1.00001	1.00046	1.00114	0.99806	0.98672	0.98789	1.04516
5.300	1.00004	1.00045	1.00065	0.99682	0.98792	0.99854	1.05671
5.350	1.00006	1.00039	1.00016	0.99605	0.99040	1.00874	1.06035
5.400	1.00007	1.00031	0.99971	0.99576	0.99376	1.01725	1.05583
5.450	1.00008	1.00021	0.99935	0.99595	0.99756	1.02312	1.04405
5.500	1.00007	1.00011	0.99909	0.99654	1.00133	1.02579	1.02694
5.550	1.00006	1.00001	0.99895	0.99744	1.00464	1.02515	1.00708
5.600	1.00005	0.99993	0.99893	0.99851	1.00715	1.02149	0.98730
5.650	1.00003	0.99986	0.99902	0.99964	1.00866	1.01546	0.97028
5.700	1.00002	0.99981	0.99919	1.00068	1.00908	1.00797	0.95812
5.750	1.00000	0.99979	0.99942	1.00156	1.00845	1.00002	0.95211
5.800	0.99999	0.99979	0.99968	1.00218	1.00692	0.99259	0.95266
5.850	0.99998	0.99981	0.99994	1.00252	1.00474	0.98655	0.95928
5.900	0.99997	0.99985	1.00018	1.00256	1.00221	0.98250	0.97073
5.950	0.99997	0.99989	1.00037	1.00233	0.99964	0.98081	0.98528
6.000	0.99997	0.99994	1.00050	1.00188	0.99730	0.98151	1.00091

we find

$$\hat{c}_1(k) = (-4\pi\lambda_1/k^3)(\sin k - k\cos k), \quad (\text{IV.9})$$

$$\hat{c}_2(k) = (-24\pi\eta\lambda_2/k^4)[2k\sin k - (k^2-2)\cos k - 2],$$
$$\quad (\text{IV.10})$$

$$\hat{c}_3(k) = (-2\pi\eta\lambda_1/k^6)[(-k^4+12k^2-24)\cos k$$
$$+ (4k^3-24k)\sin k + 24]. \quad (\text{IV.11})$$

For small values of k, we expand the trigonometric functions, obtaining

$$\hat{c}(k) = -4\pi\left[\frac{\lambda_1}{3} + 1.5\eta\lambda_2 + \frac{\lambda_1\eta}{12}\right.$$

$$\left. -k^2\left(\frac{\lambda_1}{30} + \frac{\eta\lambda_2}{6} + \frac{\eta\lambda_1}{96}\right) + O(k^4)\right]. \quad (\text{IV.12})$$

Equations (IV.7) and (IV.9)–(IV.12) are used to evaluate $\hat{G}(k)$ at 1001 evenly spaced points. The range of k is determined by the denominator of Eq. (IV.7), with the maximum value of k being chosen so that,

$$|\rho\hat{c}(k)| < 10^{-3} \quad \text{for} \quad k > k_m. \quad (\text{IV.13})$$

For values of k greater than k_m we set the denominator identically equal to one and expand $\hat{c}(k)$ in reciprocal powers of k:

$$\hat{c}(k) = \frac{A\cos k}{k^2} + \frac{B\sin k}{k^3} + \frac{D\cos k}{k^4} + \frac{E}{k^4}$$

$$+ \text{higher-order terms.} \quad (\text{IV.14})$$

The Fourier transform of $\hat{G}(k)$ is then numerically evaluated. For $0 < k < k_m$ Filon's[16] method is used. For $k > k_m$, we analytically integrate Eq. (IV.14). Retaining only the first two terms and taking the transform, we find that the remainder term becomes

$$c(r^*)_{\text{rem}} = \frac{1}{\pi r^*}\left(A\int_{k_m}^{\infty}\frac{\sin r^*k\cos k}{k}dk\right.$$

$$\left. + B\int_{k_m}^{\infty}\frac{\sin r^*k\sin k}{k^2}dk\right), \quad (\text{IV.15})$$

where

$$A = 2\lambda_1 + 12\eta\lambda_2 + \eta\lambda_1 \quad (\text{IV.16})$$

and

$$B = -2\lambda_1 - 24\eta\lambda_2 - 4\eta\lambda_1. \quad (IV.17)$$

Integration of the first integral yields,

$$\int_{k_m}^{\infty} \frac{\sin r^*k \cos k}{k} dk = \Xi - \tfrac{1}{2} Si[k_m(r^*+1)]$$

$$- \tfrac{1}{2} Si[k_m(r^*-1)], \quad (IV.18)$$

where

$$\Xi = \pi/2, \quad r^* > 1$$

$$= \pi/4, \quad r^* = 1$$

$$= 0, \quad r^* < 1. \quad (IV.19)$$

and $Si(r)$ is the sine-integral function. Integrating the second integral by parts, we get

$$\int_{k_m}^{\infty} \frac{\sin r^*k \sin k}{k^2} dk = \frac{1}{2}\left(\frac{\cos[(r^*-1)k_m]}{k_m}\right.$$

$$- \frac{\cos[(r^*+1)k_m]}{k_m} + (r^*+1)\Gamma - (r^*-1)\Delta$$

$$+ (r^*-1) Si[k_m(r^*-1)]$$

$$\left. - (r^*+1) Si[k_m(r^*+1)]\right), \quad (IV.20)$$

where

$$\Gamma = \pi/2, \quad r^* > -1$$

$$= 0, \quad r^* = -1$$

$$= -\pi/2, \quad r^* < -1, \quad (IV.21)$$

$$\Delta = \pi/2, \quad r^* > 1$$

$$= 0, \quad r^* = 1$$

$$= -\pi/2, \quad r^* < 1. \quad (IV.22)$$

The next two terms were also tested but were found to be negligible.

The greatest source of error was found to be the criterion used to obtain k_m; however, the numerical Fourier transform of $\hat{G}(k)$ and the evaluation of $Si(x)$ for large x also are significant sources of error. $Si(x)$ was evaluated by utilizing the following series expansion:

$$Si(x) = x - (x^3/3 \cdot 3!) + (x^5/5 \cdot 5!) - + \cdots. \quad (IV.23)$$

The series was terminated when the absolute magnitude of the last term was less than 10^{-6}. To check our procedure we calculated $g(r^*)$ for $r^* > 1$ at a reduced density of 0.7. The results were found to agree with those of Throop and Bearman for $1.05 < r^* < 3.95$. On the basis of this result, we surmise that the $g(r^*)$ for $r^* > 4.0$ should not be off by more than two digits in the last place. Double precision arithmetic was used throughout.

In Table VII we tabulate our results for $g(r^*)$ for $4.0 < r^* < 6.0$ and for $0.5 < \rho\sigma^3 < 1.1$.

[1] (a) J. A. Barker and D. Henderson, J. Chem. Phys. **47**, 2856 (1967); (b) **47**, 4714 (1967); (c) J. Chem. Educ. **45**, 2 (1968); (d) Can. J. Phys. **45**, 3959 (1969); (e) "Perturbation Theory and the Equation of State for Fluids," Proceedings of the Fourth Symposium of Thermophysical Properties, The American Society of Mechanical Engineers, New York, 1968, p. 30. (f) J. J. Kozak and S. A. Rice, J. Chem. Phys. **48**, 1226 (1968).

[2] P. G. Mikolaj and C. J. Pings, J. Chem. Phys. **46**, 1401 (1967). C. J. Pings, Discussions Faraday Soc. **43**, 89 (1967). P. G. Mikolaj and C. J. Pings, J. Chem. Phys. **46**, 1412 (1967). C. J. Pings, Mol. Phys. **12**, 501 (1967).

[3] S. A. Rice and P. Gray, *The Statistical Mechanics of Simple Liquids* (Interscience Publishers, Inc., New York, 1965).

[4] T. L. Hill, *Statistical Mechanics* (McGraw-Hill Book Co., New York, 1956), p. 188.

[5] (a) G. J. Throop and R. J. Bearman, Physica **32**, 1234 (1965). (b) F. Mandel and R. J. Bearman, J. Chem. Phys. **50**, 4121 (1969). (c) B. J. Alder, *ibid.* **40**, 2724 (1964).

[6] D. Levesque, Physica **32**, 1985 (1966).

[7] (a) A. A. Broyles, S. V. Chung, and H. L. Shalin, J. Chem. Phys. **37**, 2462 (1962). (b) A. A. Khan and A. A. Broyles, Phys. Rev. **134**, A367 (1964); **136**, A1260 (1964). (c) A. A. Khan and A. A. Broyles, J. Chem. Phys. **43**, 43 (1965).

[8] For Tables IVa–IVk order Document No. NAPS-00720 from ASIS National Auxiliary Publications Service, c/o CCM Information Sciences, Inc., 22 West 34th Street, New York, N.Y. 10001; remitting $1.00 for microfiche or $3.00 for photocopies.

[9] (a) L. Verlet, Phys. Rev. **159**, 98 (1967); (b) **165**, 201 (1968).

[10] L. Verlet and D. Levesque, Physica **36**, 254 (1967).

[11] J. A. Barker and D. Henderson, J. Chem. Phys. **47**, 4721 (1967).

[12] G. J. Throop and R. J. Bearman, J. Chem. Phys. **42**, 2408 (1965).

[13] A. A. Broyles, J. Chem. Phys. **35**, 493 (1961).

[14] J. K. Percus, in *The Equilibrium Theory of Classical Fluids*, H. L. Frisch and J. L. Lebowitz, Eds. (W. A. Benjamin, Inc., New York, 1964), p. II–61.

[15] R. J. Baxter, J. Chem. Phys. **47**, 4855 (1967).

[16] P. S. Davis and P. Rabinowitz, *Numerical Integration* (Blaisdell Publ. Co., Waltham, Mass., 1967), p. 62.

[17] M. S. Wertheim, Phys. Rev. Letters **10**, E501 (1963).